SCIENTIFIC REPORTS

OPEN

SUBJECT AREAS:
GRAPHENE
CATALYST SYNTHESIS

Received
18 November 2013

Accepted
20 January 2014

Published
11 February 2014

Correspondence and requests for materials should be addressed to S.W. (chmsamuel@mail.hust.edu.cn); H.R.W. (wanghairong@ncwu.edu.cn) or Y.Q.L. (liuyq@iccas.ac.cn)

Encapsulating Pd Nanoparticles in Double-Shelled Graphene@Carbon Hollow Spheres for Excellent Chemical Catalytic Property

Zheye Zhang[1], Fei Xiao[1], Jiangbo Xi[1], Tai Sun[1], Shuang Xiao[1], Hairong Wang[2], Shuai Wang[1] & Yunqi Liu[3]

[1]School of Chemistry & Chemical Engineering, Huazhong University of Science and Technology, Wuhan, 430074, P. R. China, [2]Institute of Environmental and Municipal Engineering, North China University of Water Resources and Electric Power, Zhengzhou, 450011, P. R. China, [3]Beijing National Laboratory for Molecular Sciences, Institute of Chemistry, Chinese Academy of Sciences, Beijing 100190, P. R. China.

Double-shelled hollow carbon spheres with reduced graphene oxide (RGO) as inner shell and carbon (C) layer as outer shell have been successfully designed and prepared. This tailor-making structure acts as an excellent capsule for encapsulating with ultrafine Pd nanoparticles (Pd NPs), which could effectively prevent Pd NPs from aggregation and leaching. As a result, the as-obtained RGO@Pd@C nanohybid exhibits superior and stable catalytic performance. With the aid of RGO@Pd@C, the reduction reaction of 4-nitrophenol (4-NP) to 4-aminophenol with $NaBH_4$ as reducing agent can be finished within only 30 s, even the content of Pd is as low as 0.28 wt%. As far as we know, RGO@Pd@C is one of the most effective catalyst for 4-NP reducing reaction up to now.

Noble metals have attracted considerable attention because of their potential applications in catalysis, gas sensor, energy conversion, and fuel cells[1–3]. However, the high surface energy of noble metal nanoparticals (NPs) make them easily agglomerated or shape-changed during catalytic reactions, which results in the dramatic decrease of their activity and selectivity[4,5]. To avoid aggregation, various isolated nanoreactors are employed to restrict these NPs[6–8]. Among them, the design of yolk-shell structure has been proven to be an effective strategy to prevent the aggregation of NPs. Recently, yolk/shell structured nanohybrid composed of metal particles and silica/carbon (C) shells have become the research hotspot in chemistry due to its widely applications in confined nanoreactors, catalysts and drug delivery systems[9–11]. For example, Lee and coworkers fabricated Au@SiO_2 yolk-shell nanospheres through a two-step etching treatment with potassium cyanid[12]. Liu and coworkers used dopamine as the C source and fabricated yolk-shell structured Au@C nanocomposites. Taking the advantages of C shell, the catalyst exhibited high catalytic activity, and the reduction of 4-nitrophenol (4-NP) could be finished in 5 min[13]. However, the size of metal NPs in these single-shelled structures are usually larger than 10 nm, which greatly attenuates their catalytic activity and limits their extensive application. Therefore, it is still a challenge to develop new types of yolk-shell nanostructures that can effectively prevent aggregation of NPs, retain their ultrafine particle size, and keep their high catalytic activity.

Herein, we report for the first time the design and synthesis of double-shelled reduced graphene oxide@palladium@carbon(RGO@Pd@C) hollow spheres with RGO as inner shell and amorphous C as outer shell. Graphene has been successfully utilized as a support to disperse and stabilize metal nanoparticles, because of its large surface area, extraordinary electronic transport property and strong mechanical strength[14,15]. Ultrafine Pd NPs grow well on the surface of inner shell by spontaneous redox reaction between graphene oxide (GO) and $PdCl_4^{2-}$. Moreover, the outer shell combined with inner shell can confine Pd NPs in it, which effectively prevent the aggregation and leaching of Pd NPs and increase their catalytic active area, therefore, enhance their stability and catalytic performance. Representatively, the reduction of 4-NP catalyzed by RGO@Pd@C nanocomposites can be finished within only 30 s even the content of Pd is as low as 0.28 wt%, which outperforms the catalytic activity of other reported nanocomposites[12,13].

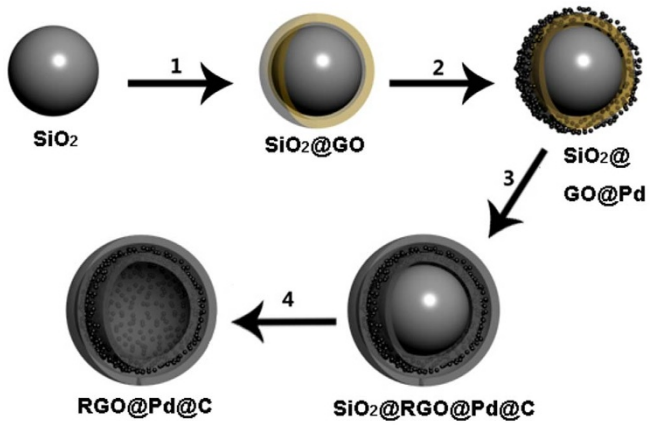

Figure 1 | Schematics of the synthesis of RGO@Pd@C hollow sphere.

Results

The synthetic procedure of RGO@Pd@C hollow spheres is illustrated in Figure 1. In step 1, SiO_2 nanospheres (100 ~ 150 nm in diameter) were firstly modified by 3-aminopropyltrimethoxysilane to introduce amine groups on their surface[16]. Then the amino-functionalized SiO_2 nanospheres were uniformly wrapped by GO layer through the electrostatic reaction and hydrogen bonds between the amino group and the oxygen-containing groups on GO sheets. Next, ultrafine Pd NPs were deposited on SiO_2@GO nanospheres by a facile and green method via a redox reaction between $PdCl_4^{2-}$ and GO in step 2[17]. In step 3, the C precursor layers were coated on the surface of the SiO_2@GO@Pd nanospheres by the pyrolysis of glucose under hydrothermal conditions[18,19]. The as-obtained product was then dried and heated at 500°C under inert atmosphere to carbonize the C precursor shell. During this process, GO layer was partially the 2D ordered structure of graphene by thermally reduction. In the final step 4, the SiO_2 cores were etched by HF solution and the double-shelled RGO@Pd@C hollow spheres were obtained.

The morphologies of the intermediate and final product were firstly characterized by transmission electron microscope (TEM). From Fig. 2A, it can be seen that SiO_2 nanospheres are tightly coated with GO film. Fig. 2B and S1 show the low and high magnification TEM images of SiO_2@GO@Pd nanospheres. Pd NPs with sizes from 1 to 2 nm are fairly well monodispersed on the surface of SiO_2@GO (Fig. S1). According to the previous studies, the reduction potential of $PdCl_4^{2-}$ is about 0.83 V vs SCE, which is higher than the oxidation potential of GO (0.48 V vs SCE). Therefore, GO/$PdCl_4^{2-}$ system can undergo spontaneous oxidation and reduction in solution[17]. The morphology of SiO_2@RGO@Pd@C is rougher than that of SiO_2@GO due to the coating of C layer. Pd NPs can be clearly observed on the surface of SiO_2@RGO@Pd@C with the sizes of 3–4 nm, which may be caused by hydrothermal treatment and followed carbonization process (Fig. 2C). After SiO_2 cores were etched with HF solution, RGO@Pd@C hollow spheres are obtained (Fig. 2D). The thickness of shells of RGO@Pd@C hollow spheres is about 10 nm based on statistical calculation from Fig. 2E. Clear wrinkles as are observed in the hollow spheres, which is one of the typical characters of RGO sheets, indicating that RGO sheets form the inner shell. Meanwhile, well-dispersed Pd NPs with an average size of 4 nm are encapsulated in the double carbon shells (Fig. S2). The interplanar spacings for the lattice fringes of Pd are 0.224 nm and 0.196 nm, which correspond to the (111) and (200) lattice planes of the face-centered cubic (fcc) Pd structure, respectively (Fig. 2F).

The microstructure of RGO@Pd@C hollow spheres was further investigated by scanning electron microscope (SEM). RGO@Pd@C hollow spheres preserve the structural integrity and spherical morphology after etching SiO_2 cores with HF solution (Fig. 3A). The size and the thickness of the RGO@Pd@C hollow spheres are quite

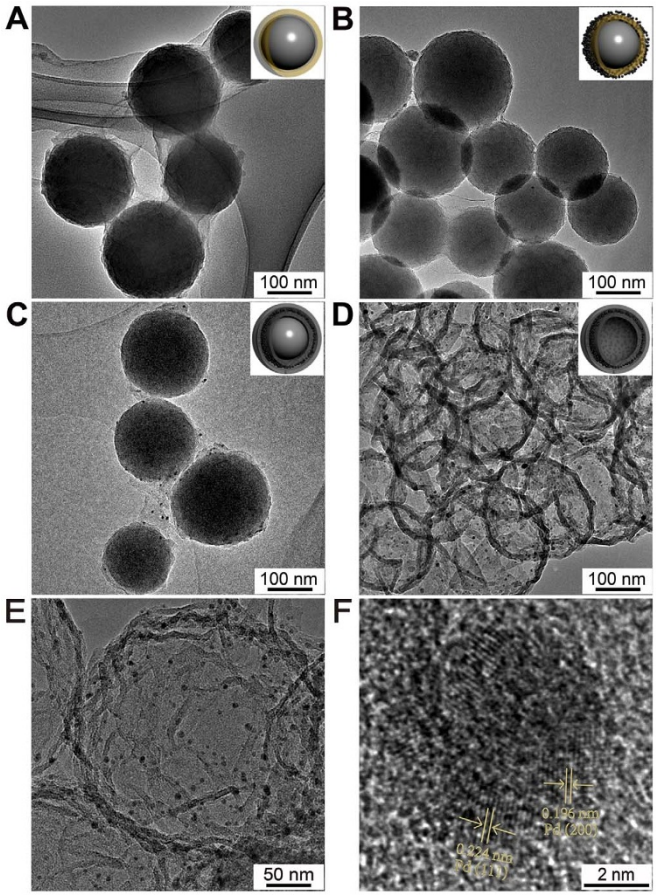

Figure 2 | TEM images of (A) SiO_2@GO nanospheres, (B) SiO_2@ GO@Pd nanospheres, (C) SiO_2@RGO@Pd@C nanospheres, (D, E) hollow RGO@Pd@C nanospheres and (F) HRTEM image of RGO@Pd@C.

uniform (Fig. 3B). The selected-area electron diffraction (SAED) pattern corresponds to the (111), (200), (220) and (311) planes of the expected fcc Pd (Fig. 3C). The X-ray photoelectron spectroscopy (XPS) of RGO@Pd@C exhibits two peaks at 335.5 eV and 340.5 eV, respectively (Fig. 3D), which are in good agreement with the reported XPS data of Pd $2p_{5/2}$ and Pd $2p_{3/2}$ in metallic Pd[20]. In addition, energy-dispersive X-ray (EDX) spectrum of composite materials also identifies the peak of Pd (Fig. S3). In comparison, RGO/Pd nanocomposites are fabricated under the same condition. But no hollow structures are formed due to the thin nanosheets of RGO can not preserve the structural integrity and spherical morphology after etching of the SiO_2 template (Fig. S4), which indicates that the outer C shell avoid the collapse of the hollow spheres.

Inspired by the high catalytic activity of Pd NPs as well as the unique structure of the double-shelled hollow spheres, we explore the applications of RGO@Pd@C as a catalyst in the reduction reaction of 4-NP to 4-AP with the aid of $NaBH_4$. It is well-known that this reaction is simple and fast in the presence of metallic surfaces[21–24]. While upon the addition of RGO@Pd@C catalysts, the reduction reaction can be finished within only 30 s. Fig. 4A shows the UV-vis spectrum changes of the reaction mixture in the presence of RGO@Pd@C catalysts. The absorption of 4-NP at 400 nm disappears quickly and absorption of 4-AP at about 300 nm peak increased accordingly. Meanwhile, the complete reduction of 4-NP to 4-AP can also be detected by color change of the solution, which changes from originally bright yellow to colorless (Fig. 4A insert). The reduction with RGO@Pd@C composite as catalyst can be done in only 30 s, even when the content of Pd in it is as low as 0.28 wt%, whereas reactions in the presence of Au@SiO_2[12], Au@C[13], Ag/

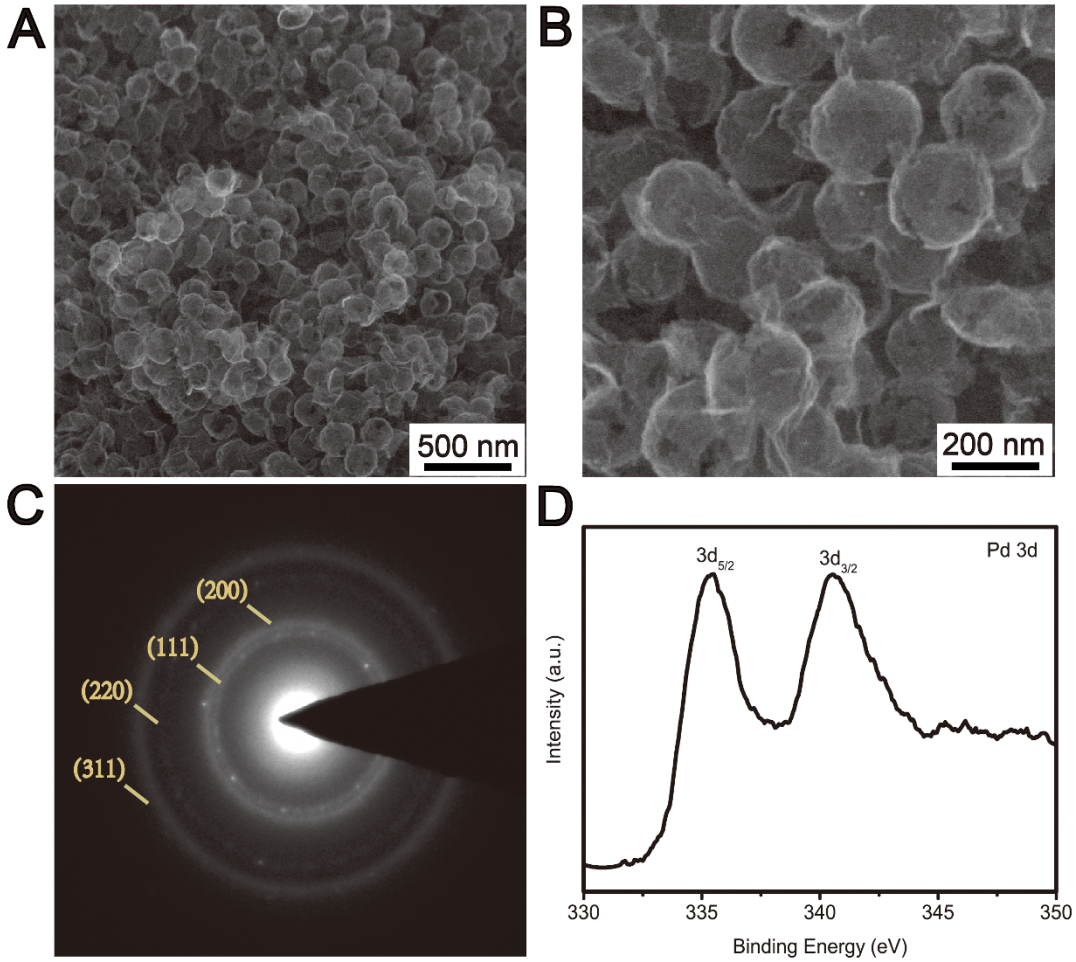

Figure 3 | (A) and (B) SEM images of RGO@Pd@C hollow spheres with different magnifications. (C) The selected-area electron diffraction (SAED) pattern and (D) XPS spectrum of Pd 3d of RGO@Pd@C.

Carbon nanofiber[25] and Au/Graphene[26] catalysts are finished more than 5 min (Table 1). Furthermore, the turnover frequency (TOF), defined as moles of the reactant (4-NP) converted by per mole of active metal in catalyst per minute, also shows much higher for RGO@Pd@C than that of Ag/Carbon nanofiber and Au/Graphene catalysts.

Discussion

The excellent catalytic performance of RGO@Pd@C composite can be ascribed to synergistic effects between Pd catalyst and double-shelled RGO@C layers. Firstly, the double-shelled RGO@C layers can effectively inhibit the aggregation and leaching of Pd NPs, and render RGO@Pd@C with high catalytic stability due to the chemical inertness and excellent mechanical stability of RGO and C shells. On the other hand, RGO can absorb 4-NP via π–π stacking interactions, and facilitate transportation of electron from RGO to Pd NPs, which to a great extent improve the catalytic performance of RGO@Pd@C nanocomposite. The stability of catalyst was investigated by repeated measurements in 4-NP under the same condition. After each measurement, the catalyst was recycled by simple

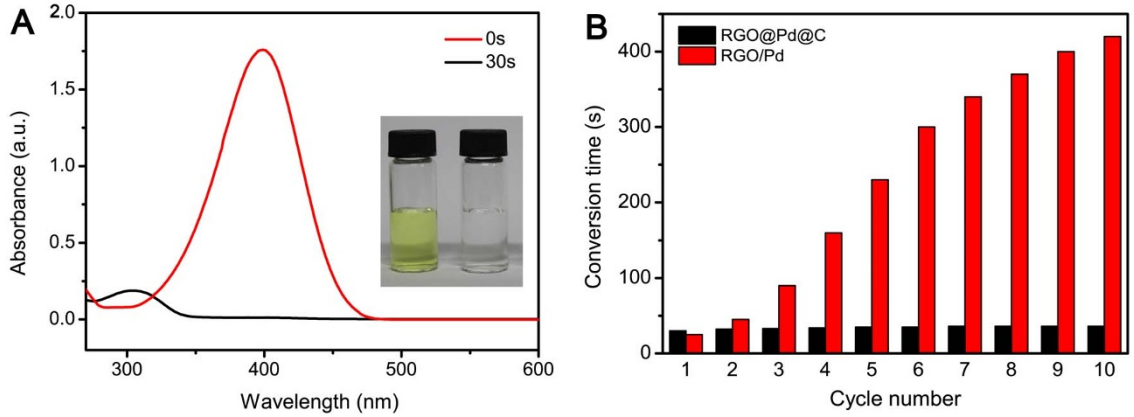

Figure 4 | (A) UV/Vis spectra of 4-NP reduction reaction in the absence and presence of RGO@Pd@C catalyst. Insert: color changes of the conversion of 4-NP. (B) The stability of catalyst by performing the same reduction reaction with 10 cycles.

Table 1 | Comparison for the reduction of 4-NP with different catalysts

Catalyst	Mass of catalyst (mg)	Amount of 4-NP (mmol)	Amount of $NaBH_4$ (mmol)	Metal size (nm)	Metal content (wt.%)	Conversion time (min)	TOF (mmol 4-NP/ (mmol metal min)	Reference
RGO@Pd@C	5	3×10^{-4}	3×10^{-2}	4	0.28	0.5	4.56	Our work
Au@C	5	3×10^{-4}	3×10^{-2}	15	NA	5	NA	13
Ag/Carbon nanofiber	1	3.6×10^{-3}	15×10^{-2}	28.1	8.4	8	0.58	25
Au/Graphene	0.1	2.8×10^{-4}	2×10^{-2}	14.6	24	12	0.19	26
Au@SiO_2	NA	3.4×10^{-3}	1.2	10^4	NA	60	NA	12

centrifugation, followed by washing with distilled water and drying in an oven overnight for the next cycle of catalysis. The catalysts exhibited well stability after 10 cycles of reactions, with 100% conversion within 40 s reaction periods. However, the reaction time increased from 25 s to 420 s under the same condition when RGO/Pd nanocomposite was used as the catalyst. (Fig. 4B). This proves that the double-shelled RGO@Pd@C hollow spheres are highly effective and stable catalysts with great potential applications.

In summary, we have developed tailor-made double-shelled hollow carbon spheres with RGO as inner shell and C layer as outer shell, which acts as an excellent capsule for encapsulating with ultrafine Pd NPs. This unique structure can effectively prevent the aggregation and leaching of Pd NPs as well as render them large active area, therefore, facilitate the high stability and catalytic performance of the nanocomposites. Using RGO@Pd@C as catalyst, the reduction of 4-NP to 4-AP could be finished in 30 s, which demonstrates that it is one of the most effective catalyst as far as we know. In addition, RGO@Pd@C also shows excellent tolerance to the chemical environment. We envision that the unique double-shelled hollow spheres will have broad applications in many fields including catalyst and drug delivery.

Methods

Synthesis of GO wrapped SiO_2(SiO_2@GO) nanospheres. GO was prepared according to a modified Hummer's method[27]. SiO_2 spheres with sizes ranging from 100 to 150 nm were purchased from Sigma-Aldrich. In a typical synthesis, 0.2 g of SiO_2 nanospheres were firstly dispersed in 100 mL ethanol by sonication for 20 min. Next, 1 mL of 3-aminopropyltrimethoxysilane was added and refluxed for 5 h to get amine-functionalized SiO_2 nanospheres. Then the products were centrifugated and rinsed with ethanol to wash away the unreacted 3-aminopropyltrimethoxysilane. After that, the 30 mL of 0.2 mg/mL GO aqueous solution was added and the mixture was stirred vigorously for 1 h. Finally, the products were collected by centrifugation, washed with water for several times, and then dried at 60°C overnight.

Synthesis of Pd NPs loaded SiO_2@GO (SiO_2@GO@Pd) nanospheres. 150 mg of as-synthesized SiO_2@GO spheres were dispersed in 60 mL of DI water, then 3 mL of 20 mM H_2PdCl_4 aqueous solution was added and the mixture was kept in a vial under vigorous stirring for 3 h in an ice bath. The products were centrifuged and washed with DI water to remove the remaining reagents followed by drying at 60°C overnight.

Synthesis of Pd NPs encapsulated double-shelled hollow carbon (RGO@Pd@C) nanospheres. 150 mg of as-prepared SiO_2@GO@Pd spheres were dispersed in 16 mL water/ethanol (volume ratio = 3/1) mixture by ultrasonication, then 4 mL of 0.5 M aqueous glucose solution was added under vigorous stirring for 30 min. After that, the suspension was transferred to a 25 mL Teflon-lined autoclave, and heated in an oven at 180°C for 16 h. The dark gray products were collected by centrifugation and washed with ethanol and DI water for six times, respectively. After drying at 60°C overnight, the resulting dark gray powder was carbonized at 500°C for 4 h under inert atmosphere. Finally, SiO_2 core was etched by HF solution (≈4%) to get RGO@Pd@C hollow spheres.

Materials characterization. The morphology and structure of products were characterized with a field-emission scanning electron microscope (SEM, FEI, Nova NanoSEM 450) and a transmission electron microscope (TEM, FEI, Tecnai G^2 20). X-ray photoelectron spectroscopy (XPS) measurements were performed on VG ESCALAB 250 spectrometer with monochromatic Al Kα (1486.71 eV) X-ray radiation (15 kV and 10 mA) and hemispherical electron energy analyzer. The UV-vis measurements were performed on a UV-2550 spectrophotometer (Shimadzu, Japan). The Pd contents in the catalysts were determined using Microwave Plasma-Atom Emission Spectrometer (MP-AES, Agilent 4100, USA).

Catalytic study. 5 mg of RGO@Pd@C nanocomposites was added to 3 mL of 1×10^{-4} M 4-NP solution. 0.1 mL 3×10^{-1} M $NaBH_4$ solution was then added with constant magnetic stirring. The changes of the reduction reaction were recorded in the UV-vis spectrophotometer.

1. Kolmakov, A., Klenov, D. O., Lilach, Y., Stemmer, S. & Moskovits, M. Enhanced Gas Sensing by Individual SnO_2 Nanowires and Nanobelts Functionalized with Pd Catalyst Particles. *Nano Lett.* **5**, 667–673 (2005).
2. Guo, S. J., Wen, D., Zhai, Y. M., Dong, S. J. & Wang, E. K. Platinum Nanoparticle Ensemble-on-Graphene Hybrid Nanosheet: One-Pot, Rapid Synthesis, and Used as New Electrode Material for Electrochemical Sensing. *ACS Nano* **4**, 3959–3968 (2010).
3. Koenigsmann, C. *et al.* Enhanced Electrocatalytic Performance of Processed, Ultrathin, Supported Pd-Pt Core-Shell Nanowire Catalysts for the Oxygen Reduction Reaction. *J. Am. Chem. Soc.* **133**, 9783–9795 (2011).
4. Narayanan, R. & El-Sayed, M. A. Effect of Catalysis on the Stability of Metallic Nanoparticles: Suzuki Reaction Catalyzed by PVP-Palladium Nanoparticles. *J. Am. Chem. Soc.* **125**, 8340–8347 (2003).
5. Narayanan, R. & El-Sayed, M. A. Catalysis with Transition Metal Nanoparticles in Colloidal Solution: Nanoparticle Shape Dependence and Stability. *J. Phys. Chem. B* **109**, 12663–12676 (2005).
6. Chen, D., Li, L. L., Tang, F. Q. & Qi, S. Facile and Scalable Synthesis of Tailored Silica "Nanorattle" Structures. *Adv. Mater.* **21**, 3804–3807 (2009).
7. Ikeda, S. *et al.* Ligand-Free Platinum Nanoparticles Encapsulated in a Hollow Porous Carbon Shell as a Highly Active Heterogeneous Hydrogenation Catalyst. *Angew. Chem. Int. Ed.* **45**, 7063–7066 (2006).
8. Kim, M., Sohn, K., Na, H. B. & Hyeon, T. Synthesis of Nanorattles Composed of Gold Nanoparticles Encapsulated in Mesoporous Carbon and Polymer Shells. *Nano Lett.* **2**, 1383–1387 (2002).
9. Kamata, K., Lu, Y. & Xia, Y. N. Synthesis and Characterization of Monodispersed Core-Shell Spherical Colloids with Movable Cores. *J. Am. Chem. Soc.* **125**, 2384–2385 (2003).
10. Cheng, D., Zhou, X., Xia, H. & Chan, H. S. O. Novel Method for the Preparation of Polymeric Hollow Nanospheres Containing Silver Cores with Different Sizes. *Chem. Mater.* **17**, 3578–3581 (2005).
11. Li, H. X. *et al.* Mesoporous Titania Spheres with Tunable Chamber Stucture and Enhanced Photocatalytic Activity. *J. Am. Chem. Soc.* **129**, 8406–8407 (2007).
12. Lee, J., Park, J. C. & Song, H. A Nanoreactor Framework of a Au@SiO_2 Yolk/Shell Structure for Catalytic Reduction of p-Nitrophenol. *Adv. Mater.* **20**, 1523–1528 (2008).
13. Liu, R. *et al.* Dopamine as a Carbon Source: The Controlled Synthesis of Hollow Carbon Spheres and Yolk-Structured Carbon Nanocomposites. *Angew. Chem. Int. Ed.* **50**, 6799–6802 (2011).
14. Goncalves, G. *et al.* Surface Modification of Graphene Nanosheets with Gold Nanoparticles: The Role of Oxygen Moieties at Graphene Surface on Gold Nucleation and Growth. *Chem. Mater.* **21**, 4796–4802 (2009).
15. Kong, B. S., Geng, J. X. & Jung, H. T. Layer-by-layer assembly of graphene and gold nanoparticles by vacuum filtration and spontaneous reduction of gold ions. *Chem. Commun.* **16**, 2174–2176 (2009).
16. Lee, J. S., You, K. H. & Park, C. B. Highly Photoactive, Low Bandgap TiO_2 Nanoparticles Wrapped by Graphene. *Adv. Mater.* **24**, 1084–1088 (2012).
17. Chen, X. M. *et al.* Synthesis of "Clean" and Well-Dispersive Pd Nanoparticles with Excellent Electrocatalytic Property on Graphene Oxide. *J. Am. Chem. Soc.* **133**, 3693–3695 (2011).
18. Lou, X. W., Li, C. M. & Archer, L. A. Designed Synthesis of Coaxial SnO_2 @carbon Hollow Nanospheres for Highly Reversible Lithium Storage. *Adv. Mater.* **21**, 2536–2539 (2009).
19. Zhang, W. M. *et al.* Tin-Nanoparticles Encapsulated in Elastic Hollow Carbon Spheres for High-Performance Anode Material in Lithium-Ion Batteries. *Adv. Mater.* **20**, 1160–1165 (2008).
20. Jin, Z., Nackashi, D., Lu, W., Kittrell, C. & Tour, J. M. Decoration, Migration, and Aggregation of Palladium Nanoparticles on Graphene Sheets. *Chem. Mater.* **22**, 5695–5699 (2010).
21. Hayakawa, K., Yoshimura, T. & Esumi, K. Preparation of Gold-Dendrimer Nanocomposites by Laser Irradiation and Their Catalytic Reduction of 4-Nitrophenol. *Langmuir* **19**, 5517–5521 (2003).
22. Panigrahi, S. *et al.* Synthesis and Size-Selective Catalysis by Supported Gold Nanoparticles: Study on Heterogeneous and Homogeneous Catalytic Process. *J. Phys. Chem. C* **111**, 4596–4605 (2007).

23. Zhang, X. & Su, Z. H. Polyelectrolyte-multilayer-supported Au@Ag core-shell nanoparticles with high catalytic activity. *Adv. Mater.* **24**, 4574–4577 (2012).
24. Li, W. Z., Kuai, L., Chen, L. & Geng, B. Y. Re-growth Etching to Large-sized Porous Gold Nanostructures. *Sci. Rep.* **3**, 2377; doi:10.1038/srep02377 (2013).
25. Zhang, P. *et al*. In situ assembly of well-dispersed Ag nanoparticles (AgNPs) on electrospun carbon nanofibers (CNFs) for catalytic reduction of 4-nitrophenol. *Nanoscale* **3**, 3357–3363 (2011).
26. Li, J., Liu, C. Y. & Liu, Y. Au/graphene hydrogel: synthesis, characterization and its use for catalytic reduction of 4-nitrophenol. *J. Mater. Chem.* **22**, 8426–8430 (2012).
27. Hummers, W. S. & Offeman, R. E. Preparation of Graphitic Oxide. *J. Am. Chem. Soc.* **80**, 1339 (1958).

Acknowledgments

This research was financially supported by the National Natural Science Foundation of China (Project No. 51173055).

Author contributions

Z.Z. and F.X. contributed equally. Z.Z., F.X., H.W., S.W. and Y.L. proposed, planned, and designed the project. Z.Z., J.X., T.S. and S.X. performed the material preparation, characterizations, and catalytic tests. All authors contributed to writing the manuscript.

Additional information

Supplementary information accompanies this paper at http://www.nature.com/scientificreports

Competing financial interests: The authors declare no competing financial interests.

How to cite this article: Zhang, Z.Y. *et al.* Encapsulating Pd Nanoparticles in Double-Shelled Graphene@Carbon Hollow Spheres for Excellent Chemical Catalytic Property. *Sci. Rep.* **4**, 4053; DOI:10.1038/srep04053 (2014).